JOURNAL OF GEOPHYSICAL RESEARCH, VOL. 113, D19203, doi:10.1029/2008JD009958, 2008

Retrieving optical depths of optically thin and mixed-phase clouds from MFRSR measurements

Tianhe Wang[1,2] and Qilong Min[1]

Received 12 February 2008; revised 13 June 2008; accepted 10 July 2008; published 9 October 2008.

[1] A new method has been developed to retrieve cloud optical depths for optically thin clouds ($\tau < 10$) from the Multifilter Rotating Shadowband Radiometer (MFRSR). On the basis of simultaneous measurements of direct and diffuse radiation from MFRSR, this method allows partition of water and ice clouds and thus improves cloud optical depth retrievals. The new retrieval algorithm achieves the high consistency of retrieved cloud optical depth from both direct-beam and total radiation: the slope of 0.95 between the two with correlation coefficient of 0.90 and RMS of 1.00. A sensitivity study illustrates that the maximum biases (relative errors) of cloud optical depth within the range of effective radius of clouds are 0.16 (4.7%) and 0.36 (8.3%) for retrievals from direct-beam radiation and from total radiation, respectively. Validation and evaluation from measurements at the Point Reyes site have been conducted, illustrating that the new retrieval algorithm provides not only accurate retrievals of cloud optical depth in terms of radiation closure but also unique mix ratio of cloud water and ice for optically thin clouds under overcast conditions. Because of the climatologic importance of thin clouds, this algorithm with unique mix ratio retrievals is important for the climate study.

Citation: Wang, T., and Q. Min (2008), Retrieving optical depths of optically thin and mixed-phase clouds from MFRSR measurements, *J. Geophys. Res.*, *113*, D19203, doi:10.1029/2008JD009958.

1. Introduction

[2] Clouds play a critical role in modulating the radiative energy in the atmosphere because of their scattering and absorption of solar and infrared radiation. Optically thin clouds in particular are climatically important as they occur frequently across the globe, and radiative flux is sensitive to small change in cloud water path (liquid and ice) when cloud water path is small [*Turner et al.*, 2007; *Min and Duan*, 2005]. Optically thin clouds can either heat or cool the atmosphere depending on their thermodynamic phase, altitude, particle size distribution, and water path. It is crucial to accurately measure cloud optical properties of optically thin clouds. However, retrievals of microphysical and optical properties for optically thin clouds are extremely challenging, as those clouds are potentially mixed phase and often broken.

[3] Various efforts have been made to derive cloud optical and microphysical properties from visible and infrared radiation measurements and from active measurements of radars and lidars [*Min and Harrison*, 1996; *Leontieva and Stamnes*, 1996; *King et al.*, 1997; *Marshak et al.*, 2000; *Sassen*, 1991; *Daniel et al.*, 2002; *Shupe et al.*, 2004; *Turner*, 2005; *Mace et al.*, 2006; *Eloranta et al.* 2006]. However, no single sensor has proven able to achieve the desired accuracy for the wide variety of atmospheric cloud situations, particularly for optically thin clouds. To face this challenge, *Min et al.* [2004a] developed a retrieval algorithm for optically thin clouds by using direct-beam measurements of narrowband spectral radiation from the Multifilter Rotating Shadowband Radiometer (MFRSR). With the correction of forward scattering of solar radiation into the instrument's field of view (FOV), the new approach substantially improves the retrieval accuracy of optical depth of thin clouds. However, using only direct-beam measurements, the approach requires a priori information about cloud thermodynamic phase or cloud-scattering phase function. Ice clouds with larger effective size and irregular shape have stronger forward scattering than water clouds. Partition of direct-beam and total radiation between two clouds of different phases would be substantially different. Incorrect assignment of cloud-scattering phase function or cloud thermodynamic phase can lead to a large error of retrieved optical depth, resulting in 5–20% error in modeled total radiation reaching the surface. The complement between information from direct-beam radiation and from total radiation allows us to distinguish cloud thermodynamic phases from simultaneous measurements of direct-beam and total radiation.

[4] The MFRSR, widely deployed over the world, is a seven-channel radiometer with six passbands of 10 nm full width at half maximum centered at 415, 500, 610, 665, 860, and 940 nm and an unfiltered silicon pyranometer [*Harrison et al.*, 1994]. It allows accurate determination of atmospheric transmittances at each passband without requiring absolute

[1] Atmospheric Science Research Center, State University of New York at Albany, Albany, New York, USA.
[2] Now at College of Atmospheric Sciences, Lanzhou University, Lanzhou, China.

0148-0227/08/2008JD009958$09.00

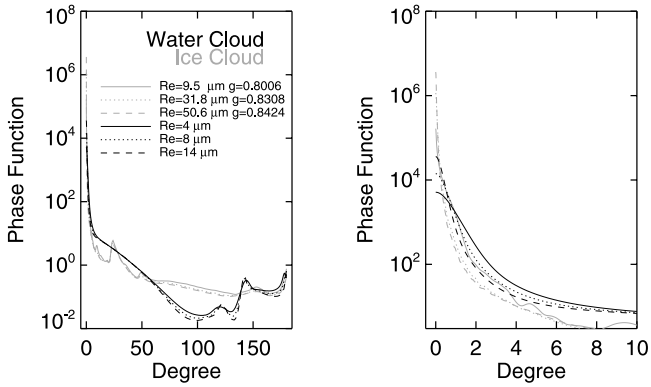

Figure 1. Water cloud and ice cloud phase functions at 415 nm for different effective radii.

calibration because it measures both total (global) horizontal irradiance and direct normal irradiance using the same detectors by a blocking technique. Langley regression of the direct normal irradiance taken on stable clear days can be used to extrapolate the instrument's response to the top of the atmosphere, and this calibration can then be applied to the total horizontal irradiance in cloud periods. Transmittances are calculated subsequently under cloudy conditions as the ratio of the uncalibrated MFRSR signal to the extrapolated top-of-atmosphere value. The uniqueness of MFRSR enables us to achieve radiation closure in terms of direct-beam and total radiation with high accuracy for a given cloud condition. In this study, we exploit the possibility of using simultaneous measurements of direct and total radiation from the same sensor, i.e., MFRSR, to determine cloud thermodynamic phases and partition of liquid and ice optical depth and thus improve retrieval accuracy of optical properties of thin clouds.

2. Cloud Phase Function and Retrieval Algorithm

[5] Optical depth of the atmosphere can be determined from measurements of transmission of the direct solar beam using Beer's law when the Sun is not fully opaque by the atmosphere. The accuracy of optical depth determined in this way is compromised by contamination of the direct transmission of light that is scattered into the sensor's FOV. This phenomenon is dominant under thin-cloud conditions, particularly in the case of cirrus clouds where strong forward scattering by ice crystals occurs. With a shadowband of 7.8°, MFRSR captures this forward-scattered radiation within its FOV in addition to the attenuated direct solar beam. The unwanted scattered radiance will result in an overestimation of the cloud transmission and will consequently result in an underestimation of the derived cloud optical depth. The forward-scattered radiation strongly depends on both phase function and optical depth of the atmospheric-scattering particles, thin clouds in this study. Figure 1 shows phase functions at 415 nm for water clouds with effective radii of 4, 8, and 14 μm and for ice clouds with effective radii of 9.5, 31.8, and 50.6 μm. Ice clouds have strong forward scattering in the forward-scattering lobe (scattering angle <10°, shown in Figure 1 (right)), which directly impacts observed direct-beam radiation. Ice clouds also have high backscattering (scattering angle >90°), which will significantly influence diffuse radiation and thus total radiation. It is clearly evident that cloud thermodynamic phase, ice or liquid, is a major factor in determining radiation partition between direct-beam and total radiation, while effective particle size of clouds within the same cloud phase play a minor role between the two. Those insights lay the foundation for our proposed retrieval algorithm.

[6] A family of retrieval algorithms has been developed for inferring cloud optical depth from MFRSR measurements: the total (diffuse) radiation algorithm [*Min and Harrison*, 1996] and the direct-beam radiation algorithm [*Min et al.*, 2004a]. These retrieval algorithms have been extensively tested and validated, demonstrating good accuracies [*Min et al.*, 2003; *Min et al.*, 2004b]. The current retrieval algorithm combines the existing algorithms in a self-consistent and systematic way. The direct-beam and total transmittances observed by MFRSR at a given cloud thermodynamic phase and optical depth, $\tau_{\mathrm{wtr,ice}}$, and effective radius, Re, can be described as follows:

$$\begin{aligned} I^{\mathrm{dir}}(\mu_0, \tau_{\mathrm{aer}}, \tau_{\mathrm{wtr,ice}}, \mathrm{Re}) &= \exp\left[-(\tau_{\mathrm{ray}} + \tau_{\mathrm{aer}} + \tau_{\mathrm{wtr,ice}})/\mu_0\right] \\ &\quad + (B_0 - B_9) \\ I^{\mathrm{tot}}(\mu_0, \tau_{\mathrm{aer}}, \tau_{\mathrm{wtr,ice}}, \mathrm{Re}) &= \mu_0 I^{\mathrm{dir}}(\mu_0, \tau_{\mathrm{aer}}, \tau_{\mathrm{wtr,ice}}, \mathrm{Re}) \\ &\quad + I^{\mathrm{dif}}(\mu_0, \tau_{\mathrm{aer}}, \tau_{\mathrm{wtr,ice}}, \mathrm{Re}), \end{aligned} \tag{1}$$

where I^{dir}, I^{dif}, and I^{tot} are the transmittances of direct normal, diffuse horizontal, and total horizontal at the cosine of solar zenith angle μ_0, respectively. Here τ_{ray} and τ_{aer} are optical depths of Rayleigh scattering and aerosols, respectively, and B_0 and B_9 are the blocked scattering radiation into the FOV at two block angles, 0° and 9°, respectively. $B_0 - B_9$ is the forward-scattering radiation presumed by the MFRSR as the direct radiation. We use a modified discrete ordinates radiative transfer (DISORT) to accurately and rapidly compute forward direct radiance and total radiation [*Min et al.*, 2004a]. On the basis of the shadowbanding geometry, we simulate the blocked forward scattering by the shadowband of MFRSR. Since effective particle size of clouds has a minor role in determining the partition of direct and total radiation, we use climatologic effective radius of clouds, 8 and 31.8 μm, as our basic set for water and ice clouds, respectively. As *Min et al.* [2004a], we take advantage of simultaneous spectral measurements of direct-beam and temporal variations to detect cloudy and aerosol periods and further separate aerosols from thin clouds on the basis of their spectral characteristics at the 415 and 860 nm channels. Unlike direct-beam radiation, the total radiation is influenced strongly by surface albedo and atmospheric absorptions. Therefore, for cloudy periods, we derive cloud optical depths from direct-beam and total radiation measurements at the 415 nm channel (equation (1)) for both water and ice cloud phases. The selection of the 415 nm channel is to avoid all gaseous absorption, except for NO_2, which has negligible impact under normal conditions. Several other factors favor the 415 nm channel compared to the 860 nm channel: when snow is absent, terrestrial albedos at 415 nm are significantly lower than at the longer wavelength and are relatively constant; the single-scattering albedo and asymmetry parameter are less sensitive to the effective radius [*Min and Harrison*, 1996].

[7] To illustrate the sensitivity of direct-beam and total radiation to cloud particle size, phase, and cloud layering, we simulate the measurements of MFRSR for various cloud

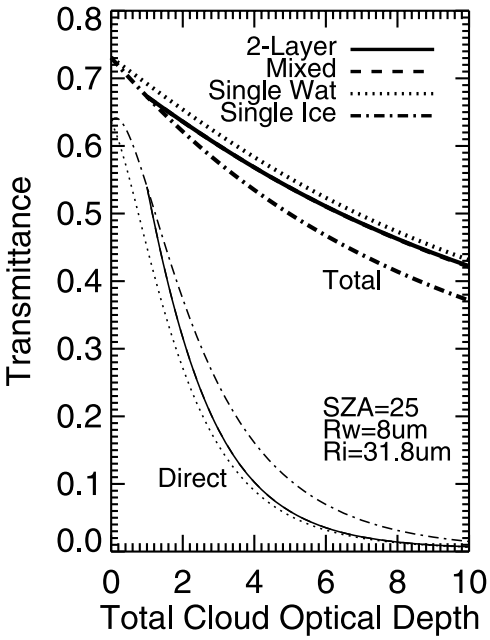

Figure 2. Simulated direct and total transmittances as a function of total cloud optical depth for pure water cloud, pure ice cloud, and two-layer (water and ice) and mixed-phase cloud systems with solar zenith angle of 25° and effective radius of 8 μm for water droplet and of 31.8 μm for ice crystal at 415 nm wavelength, respectively.

conditions. In the simulations, effective radii for water and ice clouds are assumed to be 8 and 31.8 μm, respectively. For a two-layer cloud system and a mixed-phase cloud, the optical depth of ice cloud is fixed at 1, and the optical depth of water cloud varies from 0 to 9. For the two-layer cloud system, water cloud layer and ice cloud layer are placed at 1–2 km and 5–6 km, respectively. Without accurate knowledge of optical properties of mixed-phase clouds, we used linearly weighted optical properties by optical depths of water and ice clouds to represent optical properties of mixed-phase clouds and placed the mixed-phase cloud layer at 4–6 km. Lack of atmospheric absorption at 415 nm ensures that total transmittances are insensitive to cloud layering structures. For given total cloud optical depths, the total transmittances and the direct-beam transmittances, as shown in Figure 2, are indistinguishable between a two-layer cloud system and a mixed-phase cloud. Transmittances of a two-layer cloud system and a mixed-phase cloud vary between the reference transmittances of pure water and pure ice clouds.

[8] Furthermore, under the assumption of radiation closure, we can further derive the mix ratio, α ($0 \le \alpha \le 1$), as

$$(1-\alpha)\tau_{\mathrm{wtr}}^{\mathrm{dir}} + \alpha\tau_{\mathrm{ice}}^{\mathrm{dir}} \approx (1-\alpha)\tau_{\mathrm{wtr}}^{\mathrm{tot}} + \alpha\tau_{\mathrm{ice}}^{\mathrm{tot}}, \qquad (2)$$

where $\tau_{\mathrm{wtr}}^{\mathrm{dir}}$ and $\tau_{\mathrm{wtr}}^{\mathrm{tot}}$ are retrieved cloud optical depths from direct-beam and total transmittances by assuming water cloud and $\tau_{\mathrm{ice}}^{\mathrm{dir}}$ and $\tau_{\mathrm{ice}}^{\mathrm{tot}}$ are also retrieved from the same direct-beam and total transmittances by assuming ice cloud, independently. If the mix ratio derived from equation (2) can be demonstrated to agree with the input mix ratio, the retrieval algorithm will be dramatically simplified: we only need to build up retrievals for pure water and ice cloud conditions, without dealing with various partitions of water and ice cloud optical depths. The sensitivity study below will demonstrate that equation (2) is valid and effective. The retrieval algorithms for total and direct-beam irradiance are described in detail by *Min and Harrison* [1996] and *Min et al.* [2004a], respectively. Hence, the total cloud optical depth, τ^{tot}, is

$$\tau^{\mathrm{tot}} = (1-\alpha)\tau_{\mathrm{wtr}}^{\mathrm{dir}} + \alpha\tau_{\mathrm{ice}}^{\mathrm{dir}} = (1-\alpha)\tau_{\mathrm{wtr}}^{\mathrm{tot}} + \alpha\tau_{\mathrm{ice}}^{\mathrm{tot}} \qquad (3)$$

[9] If the value of α is small ($\alpha < 0.3$), the cloud is mainly composed of water droplets; if α is large ($\alpha > 0.7$), ice crystals are dominant in the cloud. The cloud thermodynamic phase mix ratio not only distinguishes cloud thermodynamic phases but also quantitatively determines the partition of ice and water cloud optical depths for multilayer clouds or for a mixed-phase cloud. Subsequently, we can infer cloud optical depth accurately with the mix ratio information. It is worth noting that optical (and microphysical) properties of mixed-phase clouds may be substantially different from the simple linear combination of the scattering properties of water and ice clouds. The mix ratio inferred here for a single-layer cloud represents a mixed ratio of water and ice optical depths in terms of linear combination for the radiation closure.

[10] To evaluate this retrieval and assess its uncertainty, we utilize a forward radiative transfer model to simulate MFRSR measurements with prescribed cloud conditions and apply the retrieval algorithm to those simulated measurements. Figure 3 shows comparison between "true" (or input) and retrieved total cloud optical depth and mix ratio for those cases shown in Figure 2. Retrieved total cloud optical depth and mix ratio, without considering measurement error, agree well with the true values, less than 3.6% and 0.023, indicating that our retrieval method based on equation (2) is valid and effective. Real measurements always have certain degree errors. Since the accuracy of the solar constant at a nongaseous absorption channel from the Langley regression calibration is within 1% [*Michalsky et al.*, 2001], in the simulation we added ±1% measurement errors in simulated MFRSR transmittances. Given 1% measurement errors, retrieved total cloud optical depths and mix ratio vary within 8.4% and 0.107 of true corresponding values, respectively. The cloud effective particle sizes do have impact on retrievals. In our sensitivity study, four extreme sets of cloud effective sizes are tested, shown in Figure 3. Changes in cloud effective sizes have relatively large effects on mix ratio or optical depth for each phase but small effects on retrieved total optical depth (less than 0.23 at optical depth of 1 and 0.66 at optical depth of 10) because of constraints of direct-beam and total transmittances. It illustrates that this approach could provide significant improvement on retrievals of total optical depth and insensitivity to the cloud effective sizes.

3. Results

[11] Validation and evaluation of retrieved products are key to the success of a retrieval algorithm. We processed the

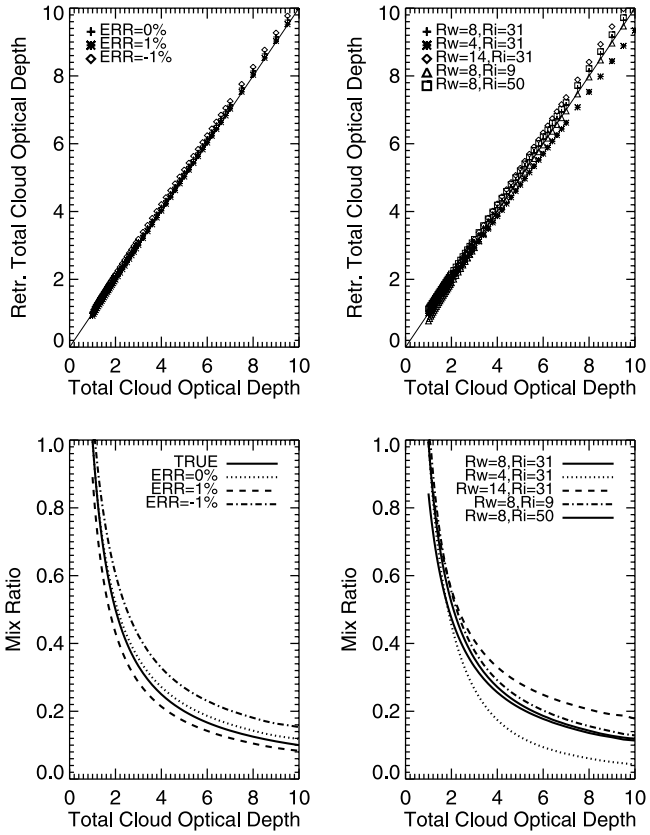

Figure 3. Comparison of cloud optical and mix ratio for those cases shown in Figure 2 between true (input) values and retrieved results and sensitivity analyses of ±1% measurement errors and four extreme sets of cloud effective sizes.

MFRSR measurements taken during the marine stratus radiation aerosol and drizzle (MASRAD) field campaign at Point Reyes, California, in 2005. Clouds observed at Point Reyes, mostly marine stratus, were often optically thin and relatively homogeneous, providing excellent conditions for evaluating our thin optical depth retrievals. Before presenting the statistical analysis for the entire field campaign we show two typical cases to demonstrate the performance of the retrievals.

[12] Since total radiation algorithm is based on the plane-parallel assumption for radiative transfer calculation, we selected cases with substantially long overcast periods to minimize 3-D effect. The 9 July 2005 case is very good, as a thin and low-level stratocumulus lasted for the entire day with few broken periods, shown in Figures 4a and 4b. Cloud physical depths detected by cloud radar were near a constant of 85 m located at 310 m with occasionally thinning periods, indicating a low-level water cloud. Cloud optical depths varied from 0.8 to 12, shown in Figure 4b. For such an optically thin low-level cloud, it is no surprise that retrieval cloud optical depths from direct-beam and total transmittance agree quite well with each other. The retrieved mix ratios (Figure 4c) are almost zero for the entire period. Thus, the cloud is classified by the algorithm as a water cloud, which is consistent with cloud radar identification. Since direct-beam and total transmittance retrieval algorithms for a single-cloud thermodynamic phase have been well validated [*Min et al.*, 2003; *Min et al.*, 2004b], with good agreement between the two in this case, we believe that the retrieved total cloud optical depths are accurate.

[13] There are a few occasions when mix ratios are above 0. Closely inspecting sky cover measured by a total sky imager (TSI) during those occasions illustrates that those periods correspond to broken cloud conditions with very thin optical depths. Diffuse (and total) radiation depends not only on optical depths of aerosols and clouds in the atmosphere but also on single-scattering properties of aerosols and clouds, largely single-scattering albedo of aerosols, especially when cloud optical depth is comparably thin to aerosol optical depth. Furthermore, 3-D inhomogeneous cloud structure violates the plane-parallel assumption of radiative transfer for diffuse radiation calculation in our retrievals, resulting in underestimation of cloud optical depth. Therefore, both aerosol loading and 3-D effect will have significant impacts on retrievals of cloud optical depth from total radiation for extremely thin clouds, which may overestimate mix ratio. For such conditions, however, we can use the direct-beam algorithm to accurately derive optical depth of optically thin clouds, as the direct-beam algorithm is insensitive to 3-D effect and aerosol single-scattering albedo [*Min et al.*, 2004a]. The cloud thermodynamic phase can be well classified under overcast conditions around the broken periods from the proposed algorithm. Furthermore, with cloud fractional cover information from other measurements and methods, for example, total sky imager, it is possible to infer an effective cloud optical depth under such broken, thin-cloud conditions from this algorithm. How to derive fractional cloud cover and improve cloud optical depth for such conditions is the subject for a future paper [*Min et al.*, 2008].

[14] The next case, 30 April 2005, is also interesting, as cloud base heights measured by the Vaisala ceilometer (VCEIL) vary from 4 km to up around the freezing level. It could be a mixed-phase or a multilayer cloud system. Unfortunately, cloud radar did not operate on that day nor did the micropulse lidar. Because of the range limitation of the VCEIL, all high cirrus clouds above 7 km cannot be detected by the VCEIL. From sky images observed by TSI, the entire day was overcast. Furthermore, our inferred optical depths are greater than 1 for the entire period. Those exclude possible clear-sky conditions during the period. Thus, those clouds without detectable cloud base by the VCEIL could be high-level ice clouds.

[15] Figure 5a shows time series of retrieved cloud optical depths from direct and total transmittance on 30 April 2005 by assuming water clouds with the effective radius of 8 μm. The difference of cloud optical depth between the two measurements varies from near zero up to 5, indicating some misclassifications of cloud thermodynamic phase. With the new retrieval algorithm, however, such differences are substantially reduced, shown in Figure 5b. The consistency of cloud optical depth ensures the radiation closure in terms of direct and total (diffuse) radiation. Consequently, the mix ratio between water and ice are derived, shown in Figure 5c. Because of the lack of direct measurement to validate inferred mix ratio, we indirectly evaluated it against

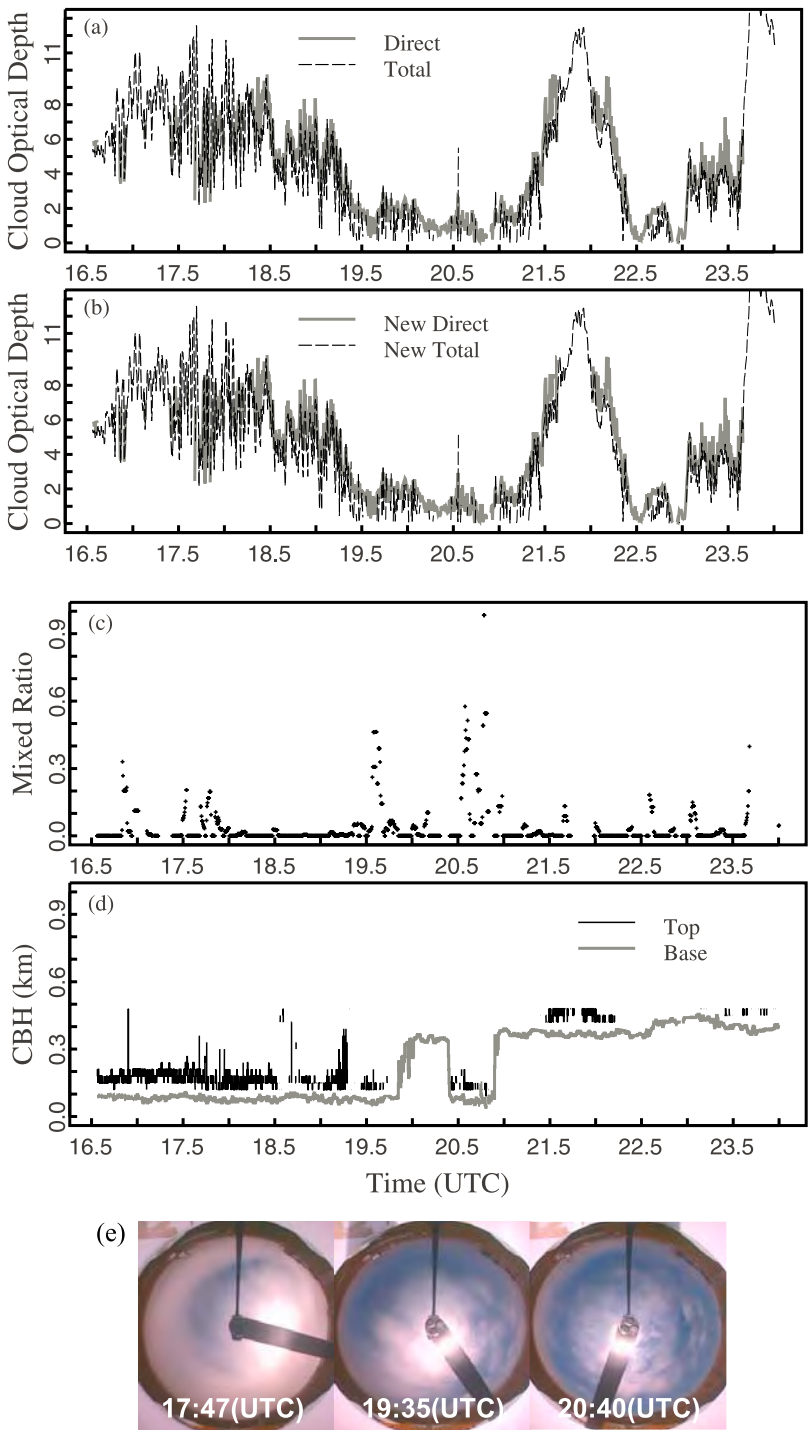

Figure 4. Cloud optical depth (COD) (a) assuming water clouds only and (b) showing new retrievals based on radiation closure on 9 July 2005 at the Point Reyes site. The gray and black lines represent COD derived from the direct radiation and from the global transmittance, respectively. (c) Mixed ratio. (d) Cloud base height (CBH) from 94 GHz Doppler radar. (e) Sky conditions from TSI.

cloud base heights detected by the VCEIL. It shows that the retrieved mix ratios from MFRSR are consistent with cloud phase conditions inferred from the VCEIL. It is worth noting that the viewing geometries of VCEIL and MFRSR are different: zenith direction for VCEIL and Sun sensor direction for MFRSR direct-beam measurements. There are slightly temporal mismatches between mix ratios and cloud base heights.

[16] For the same cloud, optical depth derived from direct-beam radiation should be close to that from total radiation. Figure 6 illustrates the improvement of the relationship between the two from assumed single-phase clouds to possible multilayer clouds or mixed-phase clouds.

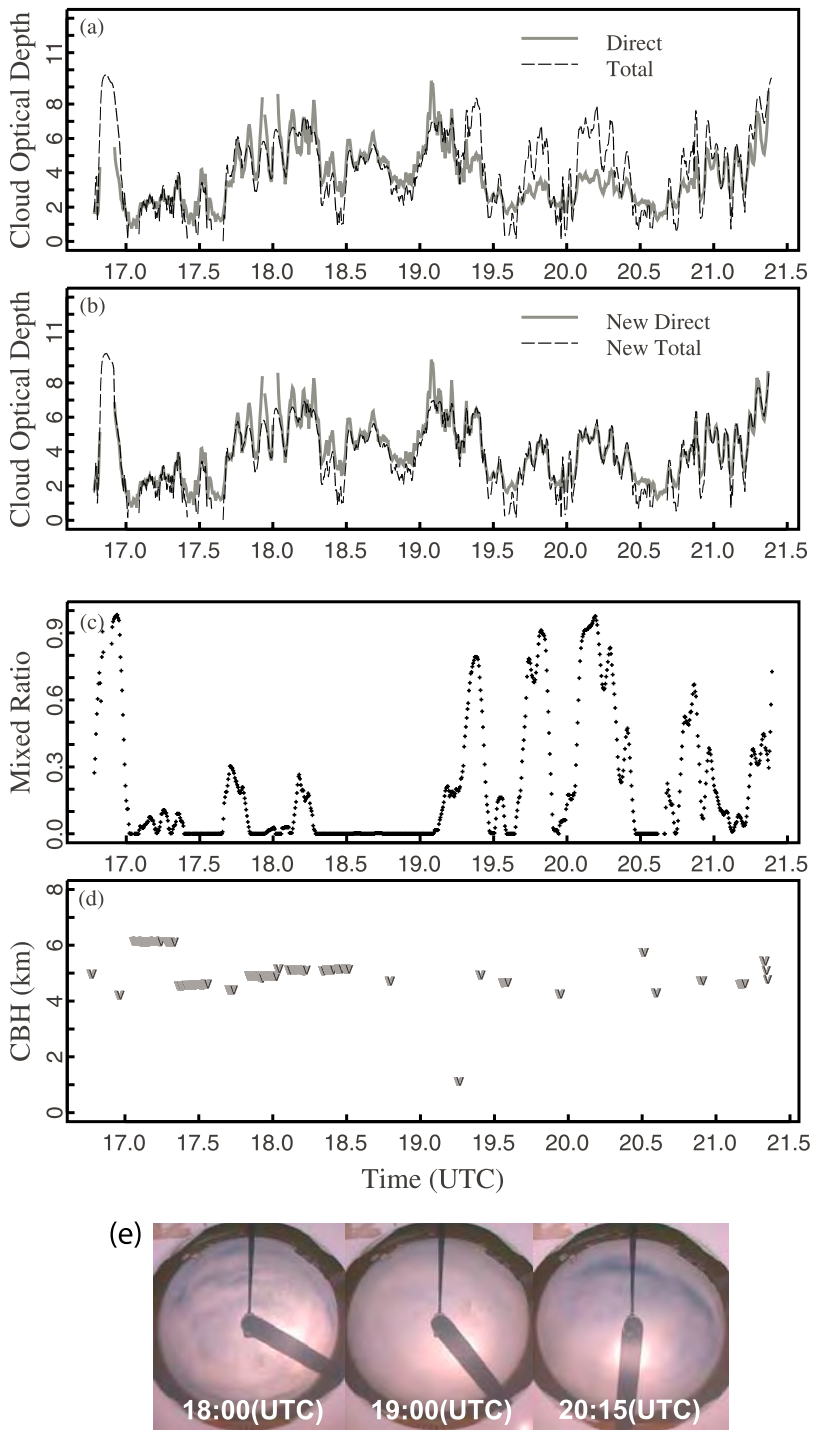

Figure 5. COD (a) assuming water clouds only and (b) showing new retrievals based on radiation closure on 30 April 2005 at the Point Reyes site. The gray and black lines represent COD derived from the direct radiation and from the global transmittance, respectively. (c) Mixed ratio. (d) CBH from VCEIL. (e) Sky conditions from TSI.

If assuming liquid phase only, the slope of scatter points (Figure 6a) is about 1.026 with correlation coefficient of 0.784. For large cloud optical depths, some retrieved values from total radiation are substantially less than those from direct-beam radiation. The reason is that assumed liquid clouds have relatively weaker forward scattering than ice clouds, resulting in underestimation of cloud optical depth from the direct-beam radiation and overestimation of cloud optical depth from the total radiation. With proper cloud phase identification, as shown in Figure 6b, the slope of the scatter points is 1.032 with a higher correlation coefficient of 0.943, and the RMS is reduced substantially from 1.26 to 0.68. This consistency of cloud optical depth will ensure the radiation closure in terms of direct and diffuse radiation.

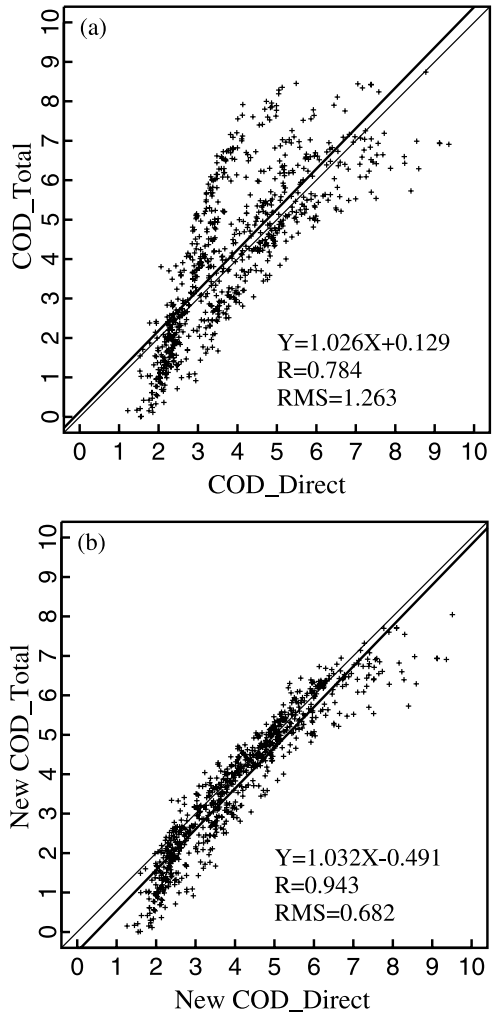

Figure 6. (a and b) Scattergrams of retrieval cloud optical depths from the direct-beam radiation and from global radiation on 30 April 2005.

[17] While the case study provides insight on the performance of this new retrieval algorithm, a more extensive evaluation is required before applying the method to various circumstances in the atmosphere. As stated previously, we selected cases (days) when substantially long periods (over 80% of a day) were overcast with optically thin clouds to minimize 3-D effects. Statistical analysis is listed in Table 1 and shown in Figure 7, which includes all 15 optically thin cloud cases that occurred during the field campaign. If assuming liquid clouds for all cases, the slope of the correlation between optical depths retrieved from direct-beam radiation and from total radiation is 0.904 with correlation coefficient of 0.81. With the new retrieval algorithm that allows cloud phase identification, the slope between the two improves to 0.95 with a higher correlation coefficient of 0.90 and a smaller RMS of 1.00. The cloud optical depths retrieved from direct-beam radiation agree well with those from total radiation in terms of radiation closure. There is still some bias in very thin optical depth regime, where optical depth derived from total radiation is low compared to that from direct-beam radiation. As discussed previously, such discrepancy may be due to 3-D effect and uncertainty associated with aerosol properties.

[18] There are some discrepancies between the total and direct-beam results (scatters of points in Figure 7b). Such a discrepancy may be introduced from following two aspects. First, 3-D effects certainly have impacts on retrievals from total radiation, even though the cases are selected on the basis of long periods of overcast conditions. A long period of overcast cannot guarantee that the cloud system satisfies the plane-parallel assumption, particularly if the cloud is a double- or multiple-layer cloud system. In addition, diffuse radiation is much smoother than direct-beam radiation because of multiple scattering [*Min et al.*, 2001]. Different smoothness scales of direct-beam and total radiation in inhomogeneous cloud field certainly result in some discrepancy of retrieved cloud optical depths. Longer time average, however, will substantially reduce such difference. Second, the retrieval algorithm of optical depth retrieval and mix ratio uses a basic set of effective sizes of 8 and 31.8 μm for liquid clouds and ice clouds, respectively. Effective particle sizes of clouds do have an impact on the scattering phase function and thus on retrieved cloud optical depths, as discussed in forward simulation tests. To assess the uncertainty associated with particle size, we tested various combinations of effective particle sizes and evaluated the impacts on the regression slope and correlation coefficient

Table 1. Comparison of Retrieval Results With Old and New Methods for the Selected 15 Optically Thin Cloud Cases

		Old Method			New Method			Mean	
Cases	Start/End Time (UT)	Slope	Intercept	R[a]	Slope	Intercept	R[a]	τ^{totb}	Alpha
20050326	1744/2252	2.663	−2.007	0.927	1.379	−0.758	0.942	1.844 (0.755)	0.416
20050416	1705/2318	0.877	0.426	0.834	0.933	−0.141	0.928	4.108 (2.080)	0.169
20050430	1647/2123	1.026	0.129	0.784	1.032	−0.491	0.943	4.155 (1.597)	0.206
20050503	1644/2334	1.317	−0.006	0.772	1.016	−0.314	0.929	4.760 (2.284)	0.421
20050629	1629/2400	0.940	−0.320	0.853	0.976	−0.665	0.886	5.025 (1.825)	0.084
20050709	1634/2400	0.902	−0.452	0.933	0.907	−0.515	0.940	4.462 (2.265)	0.036
20050713	1635/2400	1.201	−0.546	0.796	1.145	−0.770	0.840	3.083 (1.228)	0.218
20050715	1637/2400	0.889	0.053	0.882	0.930	−0.326	0.917	4.996 (2.276)	0.115
20050717	1638/2358	0.947	0.315	0.857	0.953	−0.165	0.898	4.436 (2.341)	0.214
20050726	1643/2353	0.891	0.353	0.827	0.929	−0.129	0.971	4.025 (1.883)	0.227
20050730	1646/2350	0.872	0.565	0.721	0.925	−0.169	0.841	4.473 (1.729)	0.229
20050804	1649/2346	0.949	0.677	0.803	0.976	−0.122	0.894	4.481 (1.901)	0.296
20050827	1708/2317	0.905	0.539	0.840	0.939	0	0.889	4.308 (1.762)	0.241
20050828	1710/2316	0.993	0.445	0.810	1.003	−0.205	0.910	4.210 (1.965)	0.273
20050911	1726/2250	1.095	0.125	0.832	1.011	−0.201	0.894	3.699 (1.889)	0.308

[a]R, correlation coefficient.
[b]Here τ^{tot} is total cloud optical depth with standard deviation retrieved from direct beam with the new method in parentheses.

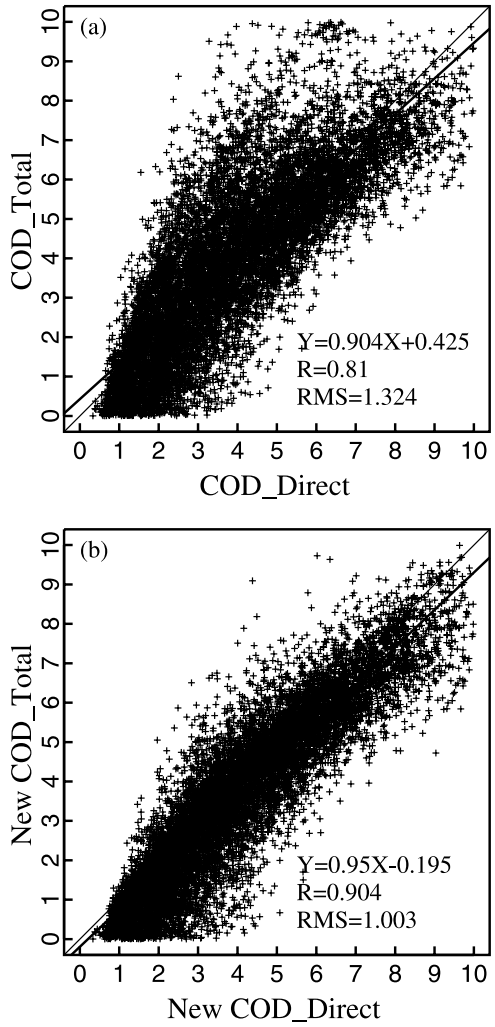

Figure 7. (a and b) Scattergrams of retrieval cloud optical depths from the direct-beam radiation and from global radiation for all cases.

for all cases. As listed in Table 2, the maximum biases (relative errors) of cloud optical depth are 0.16 (4.7%) and 0.36 (8.3%) for retrievals from direct-beam radiation and from total radiation, respectively. The effective particle size with respect to each cloud phase has a minor impact on the regression slope (from 0.925 to 0.974) and on the correlation coefficient (from 0.899 to 0.909). It demonstrates that cloud phase plays a major role in determining the partition of direct and total radiation and thus in the regression slope between cloud optical depth retrieved from the two. Uncertainty associated with cloud particle size could explain some of these discrepancies.

4. Conclusion and Discussion

[19] Optically thin clouds are climatically important. Thin clouds could either heat or cool the atmosphere depending on their thermal phase, altitude, particle size distribution, and water path. However, retrievals of microphysical and optical properties for optically thin clouds are extremely challenging. In this study, we take advantage of simultaneous spectral measurements of direct-beam and total radiation from MFRSR and utilize the difference of scattering phase function of ice and liquid clouds on the partition of direct and total radiation to derive cloud thermodynamic phase information and mix ratio and consequently to accurately infer optical depths of optically thin clouds. Specifically, we mask cloudy and aerosol periods using temporal variations of spectral radiation and further separate aerosols from thin clouds on the basis of their spectral characteristics at the 415 and 860 nm channels [*Min et al.*, 2004a]. For cloudy periods, we correct the blocked forward scattering by the shadowband of MFRSR to achieve accurate retrievals from direct-beam radiation and derive cloud optical depth from total radiation using a modified DISORT [*Min et al.*, 2004a]. Under the assumption of radiation closure, we further infer the mix ratio and identify cloud thermodynamic phases. The retrieved optical depths are, subsequently, accurate and consistent in terms of radiation closure that ensures the partition of direct and total radiation.

[20] Validation and evaluation have been done using forward simulations and the measurements from the MASRAD field campaign at Point Reyes. The new retrieval algorithm with cloud phase identification achieves the high consistency of retrieved cloud optical depth from both direct-beam and total radiation: the slope of 0.95 between the two with correlation coefficient of 0.90 and RMS of 1.00. However, there is no direct measurement of the mix ratio of multilayer clouds or mixed-phase clouds from other (passive or active) instruments so far to validate our inferred mix ratio. Evaluation against indirect information from measurements of cloud base height indicates that inferred cloud phase identification is reasonable. Because of the climatologic importance of cloud optical depth for multilayer clouds or mixed-phase clouds, the mix ratio retrieved from this algorithm is unique and important for the climate study. It is clear that the cloud thermodynamic phase is a major factor in determining radiation partition between

Table 2. The Sensitivity of Cloud Effective Radius on Cloud Optical Depth Retrievals for all Cases[a]

		τ^{dir}		τ^{tot}				
Re Water Cloud (μm)	Re Ice Cloud (μm)	$\overline{\tau - \tau_0}$[b]	Error (%)	$\overline{\tau - \tau_0}$[b]	Error (%)	Slope	Intercept	R
8	31.8	0	0	0	0	0.950	−0.195	0.904
4	31.8	0.155	4.731	0.359	8.290	0.925	−0.204	0.899
14	31.8	0.062	1.889	0.189	4.371	0.974	−0.213	0.909
8	9.5	0.093	2.816	0.102	2.349	0.936	−0.137	0.906
8	50.6	0.048	1.452	0.048	1.099	0.960	−0.243	0.905

[a]These cases include 0326, 0416, 0430, 0503, 0629, 0709, 0713, 0715, 0717, 0726, 0730, 0804, 0827, 0828, and 0911 in the 2005 year. The total number of measurements is 17,774. Re, effective radius; R, correlation coefficient.

[b]Here τ_0 is the retrieved cloud optical depth from the basis set of effective radii: 8 μm for water clouds and 31.8 μm for ice clouds.

direct-beam and total radiation, while the effective particle size of clouds within the same cloud phase plays a minor role between the two. A sensitivity study on the effective radius of clouds illustrates that the maximum biases (relative errors) of cloud optical depth within the range of effective radius of clouds are 0.16 (4.7%) and 0.36 (8.3%) for retrievals from direct-beam radiation and from total radiation, respectively. Also, 1% measurement error will result in maximum uncertainties of 8.4% and 0.107 in retrieved total cloud optical depths and mix ratio, respectively. As demonstrated, the new retrieval algorithm provides not only accurate retrievals of cloud optical depth but also unique mix ratio for optically thin clouds. It is worth noting the following issues: (1) this retrieval requires measurements of direct-beam radiation and thus is only applicable for optically thin clouds with optical depth less than 10 and (2) for extremely thin clouds (cloud optical depth comparable to aerosol optical depth) and broken clouds, optical depth derived from direct-beam radiation is accurate and should be used, and the mix ratio is not applicable. Three-dimensional effect of broken clouds and uncertainty associated with aerosol properties may compromise the retrievals from total radiation. How to derive fractional cloud cover and improve cloud optical depth for such conditions is the subject for a future paper [*Min et al.*, 2008].

[21] **Acknowledgments.** This research was supported by the Office of Science (BER), U.S. Department of Energy, grant DE-FG02-03ER63531, and by the NOAA Educational Partnership Program with Minority Serving Institutions (EPP-MSI) under cooperative agreements NA17AE1625 and NA17AE1623. Surface data were obtained from the Atmospheric Radiation Measurement (ARM) Program sponsored by the U.S. Department of Energy, Office of Energy Research, Office of Health and Environmental Research, Environmental Sciences Division.

References

Daniel, J. S., S. Solomon, R. W. Portmann, A. O. Langford, C. S. Eubank, E. G. Dutton, and W. Madsen (2002), Cloud liquid water and ice measurements from spectrally resolved near-infrared observations: A new technique, *J. Geophys. Res.*, *107*(D21), 4599, doi:10.1029/2001JD000688.

Eloranta, E. W., I. A. Razenkov, and J. P. Garcia (2006), Mixed-phase cloud measurements with the University of Wisconsin high spectral resolution lidar, paper presented at 16th Science Team Meeting, Atmos. Radiat. Meas., Albuquerque, N. M., 27–31 March.

Harrison, L. C., J. J. Michalsky, and J. Berndt (1994), Automated multifilter rotating shadowband radiometer: An instrument for optical depth and radiation measurements, *Appl. Opt.*, *33*(22), 5118–5125.

King, M. D., S. C. Tsay, S. E. Platnick, M. Wang, and K. N. Liou (1997), Cloud retrieval algorithms for MODIS: Optical thickness, effective particle radius, and thermodynamic phase, in *MODIS Algorithm Theoretical Basis Document, Rep. ATBD-MOD-05*, version 5, NASA Goddard Space Flight Cent., Greenbelt Md. (Available at http://modis.gsfc.nasa.gov/data/atbd/atbd_mod05.pdf)

Leontieva, E., and K. Stamnes (1996), Remote sensing of cloud optical properties from ground-based measurements of transmittance: A feasibility case, *J. Appl. Meteorol.*, *35*, 2011–2022, doi:10.1175/1520-0450(1996)035<2011:RSOCOP>2.0.CO;2.

Mace, G. G., et al. (2006), Cloud radiative forcing at the Atmospheric Radiation Measurement Program Climate Research Facility: 1. Technique, validation, and comparison to satellite-derived diagnostic quantities, *J. Geophys. Res.*, *111*, D11S90, doi:10.1029/2005JD005921.

Marshak, A., Y. Knyazikhin, A. B. Davis, W. J. Wiscombe, and P. Pilewskie (2000), Cloud-vegetation interaction: Use of normalized difference cloud index for estimation of cloud optical thickness, *Geophys. Res. Lett.*, *27*(12), 1695–1698, doi:10.1029/1999GL010993.

Michalsky, J. J., J. A. Schlemmer, W. E. Berkheiser, J. L. Berndt, L. C. Harrison, N. S. Laulainen, N. R. Larson, and J. C. Barnard (2001), Multiyear measurements of aerosol optical depth in the Atmospheric Radiation Measurement and Quantitative Links programs, *J. Geophys. Res.*, *106*(D11), 12,099–12,107, doi:10.1029/2001JD900096.

Min, Q., and M. Duan (2005), Simultaneously retrieving cloud optical depth and effective radius for optically thin clouds, *J. Geophys. Res.*, *110*, D21201, doi:10.1029/2005JD006136.

Min, Q., and L. C. Harrison (1996), Cloud properties derived from surface MFRSR measurements and comparison with GOES results at the ARM SGP site, *Geophys. Res. Lett.*, *23*(13), 1641–1644, doi:10.1029/96GL01488.

Min, Q., L. C. Harrison, and E. E. Clothiaux (2001), Joint statistics of photon path length and cloud optical depth: Case studies, *J. Geophys. Res.*, *106*(D7), 7375–7386.

Min, Q.-L., M. Duan, and R. Marchand (2003), Validation of surface retrieved cloud optical properties with in situ measurements at the Atmospheric Radiation Measurement Program (ARM) South Great Plains site, *J. Geophys. Res.*, *108*(D17), 4547, doi:10.1029/2003JD003385.

Min, Q., E. Joseph, and M. Duan (2004a), Retrievals of thin cloud optical depth from a multifilter rotating shadowband radiometer, *J. Geophys. Res.*, *109*, D02201, doi:10.1029/2003JD003964.

Min, Q., P. Minnis, and M. M. Khaiyer (2004b), Comparison of cirrus optical depths derived from GOES 8 and surface measurements, *J. Geophys. Res.*, *109*, D15207, doi:10.1029/2003JD004390.

Min, Q., T. Wang, C. N. Long, and M. Duan (2008), Estimating fractional sky cover from spectral measurements, *J. Geophys. Res.*, doi:10.1029/2008JD010278, in press.

Sassen, K. (1991), The polarization lidar technique for cloud research: A review and current assessment, *Bull. Am. Meteorol. Soc.*, *72*, 1848–1866, doi:10.1175/1520-0477(1991)072<1848:TPLTFC>2.0.CO;2.

Shupe, M. D., P. Kollias, S. Y. Matrosov, and T. L. Schneider (2004), Deriving mixed-phase cloud properties from Doppler radar spectra, *J. Atmos. Oceanic Technol.*, *21*(4), 660–670, doi:10.1175/1520-0426(2004)021<0660:DMCPFD>2.0.CO;2.

Turner, D. D. (2005), Arctic mixed-phase cloud properties from AERI-lidar observations: Algorithm and results from SHEBA, *J. Appl. Meteorol.*, *44*, 427–444, doi:10.1175/JAM2208.1.

Turner, D. D., et al. (2007), Thin liquid water clouds: Their importance and our challenge, *Bull. Am. Meteorol. Soc.*, *88*, 177–190, doi:10.1175/BAMS-88-2-177.

Q. Min and T. Wang, Atmospheric Science Research Center, State University of New York at Albany, Albany, NY 12203, USA. (min@asrc.cestm.albany.edu)